‘UNMIXING’ FUNCTIONAL MAGNETIC RESONANCE IMAGING WITH INDEPENDENT COMPONENT ANALYSIS

V. D. Calhoun[§ ▽ o] *and T. Adalı*[*]
[§]Olin Neuropsychiatry Research Center, Institute of Living, Hartford, CT 06106.
[▽]Dept. of Psychiatry, Yale University, New Haven, CT 06520
[o]Dept. of Psychiatry, and [†]Dept. of Radiology, Johns Hopkins University, Baltimore, MD 21205
*University of Maryland Baltimore County, Dept. of CSEE, Baltimore, MD 21250

ABSTRACT

Independent component analysis (ICA) has recently demonstrated considerable promise in characterizing fMRI data, primarily due to its intuitive nature and ability for flexible characterization of the brain function. As typically applied, spatial brain networks are assumed to be systematically non-overlapping. Often temporal coherence of brain networks is also assumed, although convolutive and other models can be utilized to relax this assumption. ICA has been successfully utilized in a number of exciting fMRI applications including the identification of various signal-types such as task and transiently task-related and physiology-related signals in the spatial or temporal domain. Additional applications include the analysis of multi-subject fMRI data, the incorporation of a priori information, and the analysis of complex-valued fMRI data. In this paper, we first introduce ICA and its application to fMRI data analysis, and then review various applications of ICA to fMRI data.

1. Introduction

What an antithetical mind! - tenderness, roughness - delicacy, coarseness - sentiment, sensuality - soaring and groveling, dirt and deity - all mixed up in that one compound of inspired clay!

-Lord Byron

Independent component analysis (ICA) is a statistical method used to discover hidden factors (sources or features) from a set of measurements or observed data such that the sources are maximally independent. Typically, it assumes a generative model where observations are assumed to be linear mixtures of independent sources, and unlike principal component analysis (PCA) which uncorrelates the data, ICA works with higher-order statistics to achieve independence.

An intuitive example of ICA can be given by a scatter-plot of two independent signals s_1 and s_2. Figure 1.1a shows a plot of the two independent signals (s_1, s_2) in a scatter-plot. Figure 1.1b and c show the projections for PCA and ICA, respectively, for a linear mixture of s_1 and s_2. PCA finds the orthogonal vectors u_1, u_2, but does not find independent vectors. In contrast, ICA is able to find the independent vectors a_1, a_2 of the linear mixed signals (s_1, s_2), and is thus able to restore the original sources.

Figure 1.1: (a) The joint density of two independent signals, (b) PCA projection (u_1, u_2), (c) ICA projection (a_1, a_2) (adopted from [1])

A typical ICA model assumes that the source signals are not observable, statistically independent and non-Gaussian, with an unknown, but linear, mixing process. Consider an

observed $M-$dimensional random vector is denoted by $\mathbf{x}=(x_1,\cdots x_M)^T$ which is generated by the ICA model:

$$\mathbf{x}=\mathbf{As} \tag{1}$$

where $\mathbf{s}=[s_1,s_{2,}...s_N]^T$ is an N-dimensional vector whose elements are assumed independent sources and $\mathbf{A}_{M\times N}$ is an unknown mixing matrix. Typically $M>=N$, so that A is usually of full rank. The goal of ICA is to estimate an unmixing matrix $\mathbf{W}_{N\times M}$ such that $\mathbf{y}$ (defined in equation (2)) is a good approximation to the 'true' sources: $\mathbf{s}$.

$$\mathbf{y}=\mathbf{Wx} \tag{2}$$

ICA is hence an approach to solve the blind source separation problem, which traditionally addresses the solution of the cocktail party problem in which several people are speaking simultaneously in the same room. The problem is to separate the voices of the different speakers, using recordings of several microphones in the room [2]. The basic ICA model for blind source separation is shown in Figure 1.2.

Figure 1.2: Basic ICA model for blind source separation

Popular approaches for performing ICA include maximization of information transfer—which is equivalent to maximum likelihood estimation, maximization of nongaussianity, mutual information minimization, and tensorial methods. The most commonly used ICA algorithms are Infomax [3], FastICA [4] and joint approximate diagonalization of eigenmatrices (JADE) [5]. The original Infomax algorithm for blind separation by [3] is better suited to estimation of super-Gaussian sources. To overcome this limitation, techniques have been developed for simultaneously separating sub- and super-Gaussian sources [6]. A flexible independent component analysis approach using generalized Gaussian density model method was introduced

in [7]. These algorithms typically work well for symmetric distributions and are less accurate for skewed distributions. Recent extensions of ICA to overcome this limitation include non-parametric ICA [8] and kernel independent component analysis [9]. Other ICA models that adaptively vary the nonlinear functions (or activation functions) to better fit the underlying sources have also been proposed [10,11]. The variety of recent approaches for performing ICA and its applications in areas as diverse as biomedicine, astrophysics, and communications demonstrates the vitality of research in this area.

2. Functional MRI

As discussed in the first article of the issue, FMRI is a technique that provides the opportunity to study brain function non-invasively and is a powerful tool utilized in both research and clinical arenas since the early 90s [12]. The most popular technique utilizes blood oxygenation level dependent (BOLD) contrast, which is based on the differing magnetic properties of oxygenated (diamagnetic) and deoxygenated (paramagnetic) blood. When brain neurons are activated, there is a resultant localized change in blood flow and oxygenation which causes a change in the MR decay parameter T_2^*. These blood flow and oxygenation (vascular or hemodynamic) changes are temporally delayed relative to the neural firing, a confounding factor known as hemodynamic lag. Scientific interest rests primarily with the electrical activity in the neurons, which cannot be directly observed by any variant of the MRI procedure. Since the hemodynamic lag varies in a complex way from tissue to tissue, and because the exact transfer mechanism between the electrical and hemodynamic processes is not known, it is not possible to completely recover the electrical process from the vascular process. Nevertheless, the vascular process remains an informative surrogate for electrical activity. However, relatively low image contrast-to-noise ratio (CNR) of the BOLD effect, head movement, and undesired physiological

sources of variability (cardiac, pulmonary) make detection of the activation-related signal changes difficult.

2.1 Data Acquisition

The MRI signal is acquired as a quadrature signal. That is, two orthogonal "detectors" are used to capture the MRI signal [13]. The two outputs from such a system are often put in a complex form, with one output being treated as the real part and the other as the imaginary part. The time-domain data acquired by the spectrometer are, remarkably, equivalent to the spatial-frequency representation of the image data, and so a discrete Fourier transform yields the complex image-space data. It is then common to take the magnitude of this data prior to performing any fMRI analyses. FMRI studies rely upon the detection of small intensity changes over time, often with a contrast-to-noise ratio of less than 1.0. Virtually all fMRI studies analyze the magnitude images from the MRI scanner. A standard approach is to correlate the time-series data with an assumed reference signal [14]. Many generalizations have been proposed, usually involving linear modeling approaches utilizing an estimate of the hemodynamic response [15]. The information contained in the phase images is ignored in such analyses.

2.2 Types of Signal and Noise

There are several types of signals that can be encoded within the hemodynamic signals measured by fMRI. Some of these were identified by McKeown in the first application of ICA to fMRI [16]. In this paper, infomax [3] was utilized and separated signals were classified as task-related, transiently task-related, and motion related.

In general, fMRI data may be grouped into signals of interest and signals not of interest. The **signals of interest** include task-related, function-related, and transiently task-related signals.

The *task-related* signal has already been mentioned and is the easiest to model. A reference waveform, based upon the paradigm, is correlated with the data. The responses of the brain to a given task may not be regular however, for example the signal may die out before the stimulation is turned off or change over time as repeated stimuli are applied, leading to a *transiently task-related* signal. It is also conceivable that there are several different types of transiently task-related signals coming from different regions of the brain. The *function-related* signal manifests as similarities between voxels within a particular functional domain (*e.g.*, the motor cortex on one side of the brain will correlate most highly with voxels in the motor cortex on the opposite side of the brain) [17]. An exciting application of this is for identifying synchronous auditory cortex activity [18,19] (see areas corresponding to the top time course in Figure 3.5). Most of these fMRI signals have been examined with ICA and other methods and have been found to be super-Gaussian in nature (except perhaps the artifacts mentioned in the next section).

The **signals not of interest** include physiology-related, motion-related, and scanner-related signals. *Physiology-related* signals such as breathing and heart rate tend to come from the brain ventricles (fluid filled regions of the brain) and areas with large blood vessels present, respectively. *Motion-related* signals can also be present and tend to be changes across large regions of the image (particularly at the edges of images). An example of a motion-related signal occurs during an experiment in which the subjects are mouthing letters, called the rapid automatized naming task [20]. Figure 2.1 depicts an example occurring during the mouthing that was extracted from orbitofrontal and inferior temporal brain regions using infomax algorithm [3]. For comparison, a typical hemodynamic response function is depicted as well. It is clear that the motion is occurring on a time scale too rapid to be related to hemodynamics. Finally, there are *scanner-related* signals that can be varying in time (such as scanner drift and system noise)

or varying in space (such as susceptibility and radio-frequency artifacts) [21]. A number of such examples can be found online including slice dropout, motion artifact, and nyquist ghosting.

Figure 2.1: Motion-related signal due to mouth movement from inferior temporal and orbitofrontal regions

There are several types of noise one can characterize in an fMRI experiment. First, there is noise due to the magnetic resonance acquisition which can be discussed as 1) object variability due to quantum thermodynamics and 2) thermal noise. It can be shown that the thermal noise will result in white noise with a constant variance in the image dimension [22]. Additionally there is noise due to patient movement, brain movement, and physiologic noise (such as heart rate, breathing). It has been suggested that physiologic noise is the dominant factor in fMRI studies [23]. In the ICA model these "noises" are often not explicitly modeled, but rather manifested as separate components, (see, e.g., [21,24]).

2.3 Statistical Properties of fMRI Data

Properties such as non-Gaussianity and spatial/temporal independence of sources need to be addressed for the application of ICA to fMRI data. If the "activations" do not have a systematic overlap in time and/or space then the distributions can be considered independent [25]. The temporal distribution of a task-related waveform is often nearly bimodal (off/on) and thus the algorithm needs to incorporate this fact. Some other basic assumptions of ICA have been considered in [16]. The assumption that components are spatially independent and add linearly was evaluated and it was concluded that the fMRI signals and noise are non-Gaussian and the accuracy of the ICA model may vary in specific regions of the brain. For example, cortex-based ICA assumes that cortical data are different from non-cortical data and processes a subset of the data determined by *a priori* information (see Section 3.6) [26]. The signals of

interest in fMRI are typically focal and thus have a super-Gaussian spatial distribution. However, the artifactual signals will be more varied and potentially sub-Gaussian.

Certain aspects of the fMRI signal are well known and could be incorporated into an ICA analysis. First, local spatial correlation exists in MR images due only to the acquisition process. It is often the case that partial k-space acquisitions involve sampling fewer frequency samples than the desired number of spatial samples. One can use the fact that the matrix of frequency data is Hermitian-symmetric to reconstruct the image using a partially acquired frequency matrix (with the trade-off being a decrease in signal-to-noise-ratio). Another well-known method involves sampling the lower frequencies and padding the high frequencies with zero (with the trade-off being a decrease in spatial resolution). This broadens the well described MRI spatial point spread function in one direction, although it has been suggested that there is a real gain in resolution when zero padding is up to as much as twice the original number of samples [27]. This results in spatial correlation of the MR signal.

In addition, spatial correlation is induced by the process being measured. The hemodynamic sources to be estimated have a spatial hemodynamic (vascular) point spread function. This is partially due to the hemodynamics, but is also a function of the pulse sequence and the parameters used. Differing degrees of sensitivity to blood flow and blood oxygenation as well as differences between low and high field magnets will measure different hemodynamics. The pulse sequence, parameters, and magnetic field strength are considered as constant to enable discussion of the hemodynamic point spread function without introducing the complexities of these parameters. There may also be some degree of temporal correlation. Temporal correlation is introduced by: 1) rapid sampling (a scanner parameter) on the time scale of the magnetic equilibrium constant, T_1 and 2) the temporal hemodynamic (vascular) point spread function (a

physiologic variable). There are also other sources of temporal autocorrelations in the data which are yet to be understood fully [28]. These data properties, which often vary from subject to subject, can impose difficulties for modeling the temporal aspects of the fMRI signal.

FMRI provides a non-invasive surrogate measure of the brain's electrical activity. It is a diverse technique and research using fMRI is growing at a rapid pace. The richness of fMRI data is only beginning to be understood. We have provided a brief introduction to the fMRI technique and summarized some of the functionally-related brain signals. It is important to understand the properties of these signals when developing methods for analyzing this data.

3. ICA of fMRI

Independent component analysis has shown to be useful for fMRI analysis for several reasons. Spatial ICA finds systematically non-overlapping, temporally coherent brain regions without constraining the temporal domain. The temporal dynamics of many fMRI experiments are difficult to study with functional magnetic resonance imaging (fMRI) due to the lack of a well-understood brain-activation model. ICA can reveal inter-subject and inter-event differences in the temporal dynamics. A strength of ICA is its ability to reveal dynamics for which a temporal model is not available [29]. Spatial ICA also works well for fMRI as it is often the case that one is interested in spatially distributed brain networks.

ICA has found a fruitful application in the analysis of fMRI data [30,31]. A principal advantage of this approach is its applicability to cognitive paradigms for which detailed a priori models of brain activity are not available. ICA has been successfully utilized in a number of exciting fMRI applications and in those that have proven challenging with the standard regression-type approaches. These include identification of various signal-types (e.g. task and transiently task-related, and physiology-related signals) in the spatial or temporal domain [32],

the analysis of multi-subject fMRI data, the incorporation of a priori information [33,34], more recently for clinical applications [35,36] and for the analysis of complex-valued fMRI data.

3.1 Spatial vs. Temporal

Independent component analysis is used in fMRI modeling to understand the spatio-temporal structure of the signal, and it can be used to discover either spatially or temporally independent components. Most applications of ICA to fMRI assume use the former approach and seek components that are maximally independent in space. In such a setting (shown in Figure 3.1), we let the observation data matrix be $\mathbf{X}$, an $N \times M$ matrix (where N is the number of time points and M is the number of voxels). The aim of fMRI component analysis is then to factor the data matrix into a product of a set of time courses and a set of spatial patterns. In principal component analysis this is achieved by singular value decomposition of the data matrix by which the data matrix is written as the outer product of a set of orthogonal, i.e., uncorrelated time courses and set of orthogonal spatial patterns. Independent component analysis takes a more general position and aims at decomposing the data matrix a product of spatial patterns and corresponding time courses where either patterns or time courses are a priori independent. ICA can also be compared with the widely used univariate general linear modeling approach which proceeds by deriving a temporal model/basis set and fitting this model to the data at each voxel by minimizing the least squared error [37]. The ICA approach does not attempt to explicitly parameterize the fMRI time course, which is estimated implicitly in the source separation algorithm (see Figure 3.1).

Since the introduction of ICA for fMRI analysis by McKeown *et al.* [24], the choice of spatial or temporal independency has been controversial. However, the two options are merely two different modeling assumptions. McKeown *et al.* argued that the sparse distributed nature of

the spatial pattern for typical cognitive activation paradigms would work well with spatial ICA (SICA). Furthermore, since the proto-typical confounds are also sparse and localized, *e.g.*, vascular pulsation (signal localized to larger veins that are moving as a result of cardiac pulsation) or breathing induced motion (signal localized to strong tissue contrast near discontinuities: "tissue edges"), the Bell-Sejnowski approach with a sparse prior is very well suited for spatial analysis [38] and has also been used for temporal ICA [25] as have decorrelation-based algorithms [38]. Stone *et al.*, proposed a method which attempts to maximize both spatial and temporal independence [39]. An interesting combination of spatial and temporal ICA was pursued by Seifritz *et al.* [18]; they used an initial SICA to reduce the spatial dimensionality of the data by locating a region of interest in which they then subsequently performed temporal ICA to study in more detail the structure of the non-trivial temporal response in the human auditory cortex.

Figure 3.1: Comparison of GLM and ICA (left) and ICA illustration (right).

3.2 A Synthesis/Analysis Model Framework

The model shown in Figure 3.2, was introduced in [40] and provides a framework for understanding ICA as applied to fMRI data and for introducing the various processing stages in ICA of fMRI data. The model assumes SICA but can be easily modified for temporal processing. A generative model is assumed for the data including the brain (in a magnet) and the fMRI scanner. Such a model provides a way to monitor the properties of the signals as they propagate through the system and to design the post-processing block, i.e., the analysis stages in a way that matches well with the properties of the source generation mechanisms. The model is also useful for validating ICA results through simulations and hybrid-fMRI data.

The *data generation block* consists of a set of statistically independent (magnetic) hemodynamic source locations in the brain (indicated by $s_i(v)$ at location v for the i^{th} source). These sources are a function of magnetic tissue properties such as T_1, T_2, T_2^*, changes in blood flow, changes in blood oxygenation, etc., that are detectable when the brain is placed in a magnetic field. The sources have weights that specify the contribution of each source to each voxel; these weights are multiplied by each source's hemodynamic time course. Finally, it is assumed that each of the N sources are added together so that a given voxel contains a mixture of the sources, each of which fluctuates according to its weighted hemodynamic time course. The first portion of the data generation block takes place within the brain in which the sources are mixed by the matrix $\mathbf{A}$. The second portion of the data generation block involves the fMRI scanner. These sources are sampled ($\mathbf{B}$) and represent a function of scan specific MR parameters such as the repeat time (TR), echo time (TE), flip angle, slice thickness, pulse sequence, field-of-view, etc.

The *data processing block* consists of a transformation, $\mathbf{T}(\cdot)$, representing a number of possible preprocessing stages, including slice phase correction, motion correction, spatial normalization and smoothing. It is common to perform a data reduction stage ($\mathbf{C}$) using PCA or some other approach. The selection of the number of sources is often done manually, but several groups have used information theoretic methods to do order selection [19,41]. The resultant estimated source, $\hat{\mathbf{s}}(j)$, along with the unmixing matrix $\hat{\mathbf{A}}^{-1}$, can then be thresholded and presented as fMRI activation images and fMRI time courses, respectively.

Figure 3.2: Model for applying ICA to fMRI data

3.3 Choice of Algorithms and Preprocessing

As mentioned in the previous subsection, ICA of fMRI involves many preprocessing stages, and there are a number of choices both for those and the ICA algorithms that can be employed. Studies of how different algorithms and preprocessing stages impact the results have been performed by several groups [40,42]. The selection of which algorithm to use will also depend upon the assumed distribution of the sources. For example, fMRI data are commonly assumed to be super-Gaussian; that is the source distributions have a heavier tail that does a Gaussian distribution. This quality can be measured using the fourth statistical moment, called kurtosis (peakedness), which is zero for a Gaussian, negative for a sub-Gaussian, and positive for a super-Gaussian distribution.

In [43], the model described in Section 3.2 was utilized to evaluate different preprocessing stages and ICA algorithms using the Kullback-Leibler (KL) divergence, a measure of the similarity between two distributions [44], as a way to determine how accurate the estimated source is compared to the "true" distribution. In the case of real fMRI data, validation is difficult as the true source distributions are unknown. However, one can move in this direction by superimposing simulated source(s) upon real fMRI data to create a "hybrid" fMRI experiment (see Figure 3.3). Sources are estimated, extracted (by ranking components by their correlation with the known sources) and compared with the actual sources. While this approach is limited, it is useful in providing a quantitative ICA performance measure. Figure 3.3 shows a thresholded "true" source (a) and its mixing function (b). Also shown is a plot of the "hybrid" fMRI data for a voxel close the "true" source maximum (c). The contrast-to-noise level is calculated as the ratio of the source amplitude to the standard deviation (over time) of a voxel within the brain. In general, it is noted that certain choices and combinations make a difference in results. In this

work, infomax outperformed (in approximation and variability) FastICA, and PCA outperformed clustering. The best overall combination for this case appears to be Infomax and PCA.

Figure 3.3: (a,b,c) Hybrid-fMRI experiment in which a known source is added to a real fMRI experiment (from [29]). (d) Comparison of algorithms and preprocessing using hybrid data.

In [45], the performance of various ICA and blind source separation algorithms is studied for application to fMRI analysis. The algorithms tested were the extended Infomax [6], FastICA [4], joint approximate diagonalization of eigenmatrices (JADE) [5], simultaneous blind extraction using cumulants (SIMBEC) [46], and AMUSE [47] in the user-friendly environment of a Matlab-based toolbox, group ICA of fMRI toolbox (GIFT) [48] incorporating the implementations from ICALAB toolbox [49]. The comparison study used both simulated fMRI-like data generated using the synthesis model shown in Figure 3.2 and actual fMRI data from seven individuals performing a four-cycle visual stimulation task.

Figure 3.4: FMRI single slice results (left visual cortex)

The experiment on simulated data included two data sets: a set of five sources and another of eight sources consisting of highly super-Gaussian, Gaussian, and sub-Gaussian sources with time courses representing sources typical to fMRI data as discussed in Section 2.2. The separation performance is measured in terms of correlation of the estimated sources with the original sources both spatially and temporally. All five algorithms were able to achieve some separation of the sources, with significant performance differences especially for the set with larger number of sources. Infomax consistently yielded reliable results, followed closely by JADE and FastICA. In the comparison with fMRI data, group ICA was performed on subjects performing an alternating left-right visuomotor task [19]. In Figure 3.4, we display that

component from the results of each algorithm which contains the left visual cortex activation from group results from three subjects. For this case, Infomax, FastICA, and JADE again successfully identify the task-related components in the left and right visual hemifields. It is also worthwhile noting that the *Z*-scores for Infomax are higher than the other algorithms for the task-related source, indicating that Infomax achieves a higher contrast to noise ratio. SIMBEC identifies the two task-related sources in the right and left hemifields; however it splits the left hemifield task-related source into two components, one of as shown in Figure 3.4 (d). AMUSE also finds the two task-related sources but places both in the same component (Figure 3.4 (e)), which might be due to the similarity of the left and right activations for the task-related source have similar spectra.

The comparisons indicate that Infomax performs most reliably, followed closely by JADE. FastICA whereas the performance of SIMBEC and AMUSE did not prove to be robust as different combination of sources and their numbers seemed to affect their performance significantly. SIMBEC, however, may prove to be useful to identify the sub-Gaussian sources, i.e., artifacts in fMRI data as its performance for these sources has been consistently very good. The performance of AMUSE is highly dependent on the differentiability of the spectra of the sources for a given delay and its performance suffers a great deal when the condition is not met.

Another approach for comparing algorithms is proposed by Esposito *et al.* in [42]. Linear correlation and receiver operating characteristics are used to compare temporal and spatial outcomes, respectively. The infomax approach appeared to be better suited to investigate activation phenomena that are not predictable or adequately modeled by inferential techniques.

3.4 Group ICA

ICA has been successfully utilized to analyze single-subject fMRI data sets, and recently extended for multi-subject analysis [19,50-52]. Unlike univariate methods (e.g., regression analysis, Kolmogorov-Smirnov statistics), ICA does not naturally generalize to a method suitable for drawing inferences about groups of subjects. For example, when using the general linear model, the investigator specifies the regressors of interest, and so drawing inferences about group data comes naturally, since all individuals in the group share the same regressors. In ICA, by contrast, different individuals in the group will have different time courses, and they will be sorted differently, so it is not immediately clear how to draw inferences about group data using ICA.

An approach was developed for performing an ICA analysis on a group of subjects [19] which extends the synthesis/analysis model mentioned in Section 3.2. In order to reduce computational load, data reduction was first performed for each subject's data then a second, aggregate model order reduction was performed. Back-reconstruction and statistical comparison of individual maps and time courses is performed following the ICA estimation. This approach is implemented in a Matlab toolbox [48].

Group maps for an ICA analysis of a four cycle alternating left/right visual stimulation task collected from a 1.5T Phillips scanner are presented in Figure 3.5. The number of components is estimated to be twenty-one by the two information-theoretic criteria employed: the minimum description length and Akaike's information criterion. Thus, the aggregate data are reduced to this dimension and twenty-one components were estimated. Both maps are thresholded at $p < 0.001$ ($t = 4.5$, $df = 8$). Several interesting components were identified within the data. Separate components for primary visual areas on the left and the right visual cortex (depicted in

red and blue, respectively) were consistently task-related with respect to the appropriate stimulus. A large region (depicted in green) including occipital areas and extending into parietal areas appeared to be sensitive to changes in the visual stimuli. Additionally some visual association areas (depicted in white) had time courses which were not task related. A comparison of group ICA approaches is found in [53].

Figure 3.5: fMRI Group ICA results (from [19])

Higher order tensor decompositions (also known as multidimensional, multi-way, or n-way), probably the first class of algorithms that performed ICA successfully [54], have received renewed interest recently, although their adaptation to group and multi-group fMRI data is still being explored. Recently, a tensorial approach was developed to estimate a single spatial, temporal, and subject-specific 'mode' for each component to attempt to capture the multidimensional structure of the data in the estimation stage [55].

3.5 Multiple Groups

In many fMRI experiments, it is desirable to directly compare and contrast two different conditions either within or between subject groups. Methods for performing such comparisons have been developed within the framework of the general linear model; however such comparisons are not intuitive for ICA. Comparisons of two ICA groups can be problematic because the ICA results represent a comparison of two different linear models with different time courses. A method for performing subtractive and conjunctive comparisons of group ICA data is proposed in [56]. An alternative method is given in [57]. One solution involves extracting components of interest using an *a priori* spatial or temporal template and quantifying whether the components extracted from the two groups have sufficiently unique time courses from the

remaining components. An analysis of seven participants performing three paradigms (each was a four cycle alternating left/right paradigm in which either visual, motor, or both visual and motor stimuli were used) can then be compared between paradigms as seen in Figure 3.6.

Figure 3.6: Visual, motor, and visuomotor data comparisons (from [58])

Additional parameterizations are also possible. For example in this study onset latencies were estimated using a weighted least squares technique [59]. A small, but significant latency difference was observed between the onset of visual and motor activation. Such an approach allows comparisons of both brain activation and time course parameters across paradigms for the flexible modeling approach, ICA.

3.6 Applications to Clinical Research

ICA has more recently been applied to address some clinically relevant questions [60]. For example, ICA has been used to study differences in brain activation due to pain in healthy individuals vs. those with chronic pain [61] and even to distinguish between Alzhiemer's patients and healthy controls by examination of the brain's 'default mode' estimated using ICA [35,62]. In this section, we give a couple examples from our own work. We first discuss using ICA to classify schizophrenia patients from healthy controls. Next, we discuss briefly the use of the simulated driving paradigm to study the impact of alcohol intoxication at two doses upon fMRI data.

3.6.1 Classification of Schizophrenia

Among the most prominent features of schizophrenia brains are abnormalities in temporal lobe structure and function; in particular in the superior temporal gyrus (STG). In this study, we attempted to examine temporal lobe function utilizing an intrinsic, task-uncorrelated measure.

Using functional magnetic resonance imaging data collected from a 1.5T GE Scanner, we calculated synchronous hemodynamic independent maps (SHIMs) of temporal lobe in 17 patients and 17 matched controls while they performed an auditory oddball task (for more details see [36]). These maps are computed using ICA, which resulted in one of the components showing large values in superior temporal lobe. Patient SHIMs revealed greater synchrony in anterior and lateral STG regions; control SHIMs had greater synchrony in posterior and medial regions. Right auditory cortex difference maps indicate regions where controls > patients (orange) and where patients > controls (blue) [see Figure 3.7, right]. Also shown are boundaries (in green and yellow) depicting intra-individual comparison regions determined by thresholding difference maps that maximized discrimination between the 2 groups.

Figure 3.7: (left) Mean activation maps from patients with schizophrenia and healthy controls.

A within-participant subtractive comparison of these two sets of right hemisphere temporal lobe regions (optimized for cohort 1 using a minimum probability of error criterion) differentiated schizophrenia from healthy controls with 97% accuracy initially (further validated by a re-test of the healthy controls) and performed with 94% accuracy in a confirmatory study of new subjects scanned at a different site. These results shed new light on STG functional differences in schizophrenia, suggest that aberrant patterns of coherence in temporal lobe cortical regions are a cardinal abnormality in schizophrenia, and have the potential to provide a powerful, quantitative clinical tool for the assessment of schizophrenia.

3.6.2 Alcohol Intoxication Studies

More recently, we, and others, have used ICA to decompose fMRI data sets acquired during naturalistic viewing paradigms [29,63]. Such conditions naturally lend themselves to an

ICA analysis since the temporal dynamics are largely unknown in such cases. It is then possible to study deviations of such decompositions due to medication or drugs. We investigated impaired driving using a simulated driving skill game that presents an “in-car” view of a road and a speed readout by alternating between fixation, driving, and watching [29,64]. We explored behavioral alterations and fMRI activation at two blood alcohol concentrations (BACs, 0.04 and 0.08 and placebo). Scanning occurred on a 1.5T Philips MRI scanner. Imaging results demonstrated seven separate networks of brain networks with different time courses (see Figure 3.8). For this analysis, the ICA spatial maps were estimated from the placebo condition, “fixed”, and time courses were then estimated from all the data.

A global disruptive effect of alcohol was observed. In addition, dose-dependent fMRI changes were revealed in orbitofrontal and motor (but not cerebellar) regions; visual and medial frontal regions were unaffected. Cerebellar regions were significantly associated with driving behavior in a dose-dependent manner. ICA was thus used to determine that alcohol demonstrated unique, disruptive, dose-dependent effects on fMRI signal within several brain circuits. This work has enabled us to build a model for how brain activity is stimulated by simulated driving, and is impacted by various factors such as alcohol and speed.

Figure 3.8: Driving-related networks and their associated time courses compared while sober and at two doses of alcohol.

3.7 Incorporation of Prior Information

The incorporation of prior information into ICA methods is important as it can provide improved separability and allow *selective* exploratory analysis. In addition, ICA methods make assumptions about, e.g. the distributional shape of the sources, and thus it is important to both assess the impact of such assumptions and modify them based upon given fMRI data.

There have been a number of applications of ICA that have attempted to utilize prior information for fMRI analysis. For example, using a reference function to extract only a single component is proposed in [65]. A more general Lagrange-based approach for constraining the spatial sources is found in [66]. Stone *et al.* propose a skewed symmetric nonlinearity (i.e., assume that the source distributions are skewed). This makes sense if one is interested in components that consist largely of either activations or deactivations [67]. Formisano *et al.* propose performing ICA upon data extracted from the cortex (where the activation is expected to be occurring) using a tessellation model of the brain cortex derived from a high resolution structural image [26]. Duann *et al.* examine time-locked temporal structure and propose a visualization approach to evaluate trial-by-trial variability [68]. An advanced mean field approach was invoked for handling situations with adaptive binary source signals [69]. In temporal mode this method can separate on/off signals while in spatial mode the approach leads to an algorithm that shares many features with Fuzzy clustering. Bayesian methods provide a useful way to incorporate prior information into ICA and may prove useful for fMRI analysis [70].

3.7.1 Spatial Prior Information

The successful applications of ICA to fMRI signals are dependent on the validity of the statistical assumptions implicit in the method. In fMRI data, the physiological signals of interest are governed by a small percentage of the whole brain map, whereas the majority of brain regions are governed by less significant homogeneous background with signal of non-interest in the task-related activation maps. While conventional ICA approaches, including a fixed nonlinear function-based algorithm or a high-order cumulant-based algorithm, work well in highly kurtotic or super-Gaussian and sub-Gaussian sources, they might provide poor results

with fMRI data due to their lack sensitivity to such specifically skewed distributions and low kurtotic signals. We recently proposed a source density-driven optimal ICA method, aiming to incorporate physically realistic assumptions and a more flexible nonlinearity to improve separation results [71]. Our method provides comparable performance to a flexible gaussian mixture, expectation-maximization based approach with much less computation complexity [72].

The central idea is to use a two-stage separation process: 1) Conventional ICA used for all channel sources to obtain initial independent source estimates; 2) source estimate-based "optimal" nonlinearities used for the "refitting" separation to all channel sources. The ICA algorithm is not based on fixed nonlinear functions, but on flexible nonlinearities of density matched candidates. The performance of ICA can be improved by seeking "matched" nonlinearities for each source and incorporating *prior* information into the ICA algorithm. Figure 3.9 shows the comparison between optimal ICA and Infomax ICA on the fMRI visual stimulation data of a single subject.

Figure 3.9: Comparison between Source Density-Driven ICA and Infomax ICA

3.7.2 Temporal Prior Information

It is also useful to impose constrains directly upon the mixing matrix in a spatial ICA fMRI analysis. For example, a component selective constraint of the ICA model mixing matrix such that one or more specific components are constrained to be "close" to a paradigm-derived time course is shown in Figure 3.10 [33]. The degree of closeness is specified by the user based upon amount of confidence placed in the information provided. Such an approach can also be formulated using a Lagrange framework. Results from our approach are shown below for an

fMRI experiment for an auditory detection task. The participant was responding to the target with a button press.

Figure 3.10: Comparison of ICA and sbICA in one participant

The left side of the figure demonstrates the task-related component for an unconstrained ICA analysis. On the right is the constrained (or semi-blind) analysis showing additional regions including motor cortex towards the top of the figure [33]. The temporal correlation with the paradigm is much higher for the constrained analysis as expected. These results demonstrate the utility of incorporating mixing matrix constraints in an fMRI analysis.

3.8 Complex Images

Functional magnetic resonance imaging (fMRI) is a technique that produces complex-valued data; however the vast majority of fMRI analyses utilize only magnitude images despite the fact that the phase information has a straightforward physiologic interpretation [73]. A number of ICA algorithms are extended to the complex domain and can be utilized for processing the fMRI data in its native complex domain. The performance of the complex infomax algorithm that uses an analytic (and hence unbounded) nonlinearity with the traditional complex infomax approaches that employ bounded (and hence non-analytic) nonlinearities as well as with a cumulant-based approach has been studied [74]. Results from a magnitude-only and complex-valued analysis are presented in Figure 3.11. The complex-valued approach results in a larger contiguously activated region in all subjects (from [75]). In addition, the phase information is captured by the complex-valued approach (c,d).

Figure 3.11: Results from magnitude-only analysis (a) and complex-valued analysis (b,c,d).

4. CONCLUSION

The application of ICA to fMRI data has proved to be quite fruitful. However there is still much work to be done in order to take full advantage of the information contained in the data. Additional prior information about multiple expected sources (both interesting and non-interesting) and their properties (fMRI properties, physiologic recording, etc) can be utilized. In addition to incorporating appropriate assumptions (and moving towards a semi-blind source separation) it is important to relax inappropriate assumptions (such as having a fixed temporal delay for each source). One of the strengths of ICA of fMRI is its ability to characterize the high-dimensional data in a concise manner. Continuing to do this and developing ways to mine the unexpected information in fMRI data will provide an exciting future for ICA of fMRI.

5. REFERENCES

[1] A. Jung, "An Introduction to a New Data Analysis Tool: Independent Component Analysis," in *Proc. Workshop GK "Nonlinearity"*, 2001.

[2] A. Hyvärinen, "Survey on Independent Componenet Analysis," *Neural Computing Surveys*, vol. 2, pp. 94-128, 1999.

[3] A. J. Bell and T. J. Sejnowski, "An Information Maximisation Approach to Blind Separation and Blind Deconvolution," *Neural Comput.*, vol. 7, pp. 1129-1159, 1995.

[4] A. Hyvarinen and E. Oja, "A Fast Fixed-Point Algorithm for Independent Component Analysis," *Neural Comput.*, vol. 9, pp. 1483-1492, 1997.

[5] J. F. Cardoso and A. Souloumiac, "Blind Beamforming for Non Gaussian Signals," *IEE-Proceeding-F*, vol. 140, pp. 362-370, 1993.

[6] T. W. Lee, M. Girolami, and T. J. Sejnowski, "Independent Component Analysis Using an Extended Infomax Algorithm for Mixed Subgaussian and Supergaussian Sources," *Neural Comput.*, vol. 11, pp. 417-441, 1999.

[7] S. Choi, A. Cichocki, and S. I. Amari, "Flexible Independent Component Analysis," *Journal of VLSI Signal Processing*, vol. 26, pp. 25-38, 2000.

[8] R. H. Boscolo, H. Pan, and V. P. Roychowdhury, "Non-Parametric ICA.," in *Proc. Int. Conf. on ICA and BSS*, 2001.

[9] F. Bach and M. Jordan, "Kernel Independent Component Analysis," *Journal of Machine Learning Research*, vol. 3, pp. 1-48, 2002.

[10] N. Vlassis and Y. Motomura, "Efficient Source Adaptivity in Independent in Independent Component Analysis," *IEEE Trans. Neural Networks*, vol. 12, pp. 559-566, 2001.

[11] B. Hong, G. D. Pearlson, E. Egolf, and V. D. Calhoun, "Identification of Brain Activity in a Visual Stimulation Task - An Adaptive ICA Approach for FMRI Data," in *Proc. HBM*, 2004.

[12] K. K. Kwong, J. W. Belliveau, D. A. Chesler, I. E. Goldberg, R. M. Weisskoff, B. P. Poncelet, D. N. Kennedy, B. E. Hoppel, M. S. Cohen, and R. Turner, "Dynamic Magnetic Resonance Imaging of Human Brain Activity During Primary Sensory Stimulation," *Proc. Natl. Acad. Sci.*, vol. 89, pp. 5675-5679, 1992.

[13] D. I. Hoult, C. N. Chen, and V. J. Sank, "Quadrature Detection in the Laboratory Frame," *Magn. Res. Med.*, vol. 1, pp. 339-353, 1984.

[14] P. A. Bandettini, A. Jesmanowicz, E. C. Wong, and J. S. Hyde, "Processing Strategies for Time-Course Data Sets in Functional MRI of the Human Brain," *Magn. Res. Med.*, vol. 30, pp. 161-173, 1993.
[15] K. J. Worsley and K. J. Friston, "Analysis of FMRI Time-Series Revisited--Again," *NeuroImage*, vol. 2, pp. 173-181, 1995.
[16] M. J. McKeown and T. J. Sejnowski, "Independent Component Analysis of FMRI Data: Examining the Assumptions," *Hum. Brain Map.*, vol. 6, pp. 368-372, 1998.
[17] B. Biswal, F. Z. Yetkin, V. M. Haughton, and J. S. Hyde, "Functional Connectivity in the Motor Cortex of Resting Human Brain Using Echo-Planar MRI," *Magn. Res. Med.*, vol. 34, pp. 537-541, 1995.
[18] E. Seifritz, F. Esposito, F. Hennel, H. Mustovic, J. g. Neuhoff, D. Bilecen, G. Tedeschi, K. Scheffler, and F. D. Salle, "Spatiotemporal Pattern of Neural Processing in the Human Auditory Cortex," *Science*, vol. 297, pp. 1706-1708, 2002.
[19] V. D. Calhoun, T. Adali, G. D. Pearlson, and J. J. Pekar, "A Method for Making Group Inferences From Functional MRI Data Using Independent Component Analysis," *Hum. Brain Map.*, vol. 14, pp. 140-151, 2001.
[20] M. B. Denckla, "Performance on Color Tasks in Kindergarten Children," *Cortex*, vol. 8, pp. 177-190, 1972.
[21] C. F. Beckmann, J. A. Noble, and S. M. Smith, "Artefact Detection in FMRI Data Using Independent Component Analysis," in *NeuroImage*, vol. 11, p. S614, 2000.
[22] Y. Wang, MR Image Statistics and Model-Based MR Image Analysis, PhD. Dissertation, *UMBC*, 1995.
[23] G. Kruger and G. H. Glover, "Physiological Noise in Oxygenation-Sensitive Magnetic Resonance Imaging," *Magn Reson. Med.*, vol. 46, pp. 631-637, 2001.
[24] M. J. McKeown, S. Makeig, G. G. Brown, T. P. Jung, S. S. Kindermann, A. J. Bell, and T. J. Sejnowski, "Analysis of FMRI Data by Blind Separation Into Independent Spatial Components," *Hum. Brain Map.*, vol. 6, pp. 160-188, 1998.
[25] V. D. Calhoun, T. Adali, G. D. Pearlson, and J. J. Pekar, "Spatial and Temporal Independent Component Analysis of Functional MRI Data Containing a Pair of Task-Related Waveforms," *Hum. Brain Map.*, vol. 13, pp. 43-53, 2001.
[26] E. Formisano, F. Esposito, F. D. Salle, and R. Goebel, "Cortex-Based Independent Component Analysis," in *NeuroImage*, vol. 13, p. S199, 2001.
[27] R. T. Constable, I. Kay, M. R. Smith, and R. M. Henkelman, "High Quality Zoomed MR Images," *J. Comput. Assist. Tomogr.*, vol. 13, pp. 179-181, 1989.
[28] E. Zarahn, G. K. Aguirre, and M. D'Esposito, "Empirical Analyses of BOLD FMRI Statistics. I. Spatially Unsmoothed Data Collected Under Null-Hypothesis Conditions," *NeuroImage*, vol. 5, pp. 179-197, 1997.
[29] V. D. Calhoun, J. J. Pekar, V. B. McGinty, T. Adali, T. D. Watson, and G. D. Pearlson, "Different Activation Dynamics in Multiple Neural Systems During Simulated Driving," *Hum. Brain Map.*, vol. 16, pp. 158-167, 2002.
[30] V. D. Calhoun, T. Adali, J. C. Hansen, J. Larsen, and J. J. Pekar, "ICA of FMRI: An Overview," in *Proc. Int. Conf. on ICA and BSS*, Nara, Japan, 2003.
[31] M. J. McKeown, L. K. Hansen, and T. J. Sejnowsk, "Independent Component Analysis of Functional MRI: What Is Signal and What Is Noise?," *Curr. Opin. Neurobiol.*, vol. 13, pp. 620-629, 2003.
[32] T. P. Jung, S. Makeig, M. Westerfield, J. Townsend, E. Courchesne, and T. J. Sejnowski, "Analysis and Visualization of Single-Trial Event-Related Potentials," *Hum. Brain Mapp.*, vol. 14, pp. 166-185, 2001.
[33] V. D. Calhoun, T. Adali, M. Stevens, K. A. Kiehl, and J. J. Pekar, "Semi-Blind ICA of FMRI: A Method for Utilizing Hypothesis-Derived Time Courses in a Spatial ICA Analysis," *NeuroImage*, vol. 25, pp. 527-538, 2005.
[34] C. F. Beckmann and S. M. Smith, "Probabilistic Independent Component Analysis for Functional Magnetic Resonance Imaging," *IEEE Trans. Med. Imaging*, vol. 23, pp. 137-152, 2004.
[35] M. D. Greicius, G. Srivastava, A. L. Reiss, and V. Menon, "Default-Mode Network Activity Distinguishes Alzheimer's Disease From Healthy Aging: Evidence From Functional MRI," *Proc. Natl. Acad. Sci. U. S. A*, vol. 101, pp. 4637-4642, 2004.
[36] V. D. Calhoun, K. A. Kiehl, P. F. Liddle, and G. D. Pearlson, "Aberrant Localization of Synchronous Hemodynamic Activity in Auditory Cortex Reliably Characterizes Schizophrenia," *Biol. Psychiatry*, vol. 55, pp. 842-849, 2004.

[37] K. J. Friston, P. Fletcher, O. Josephs, A. Holmes, M. D. Rugg, and R. Turner, "Event-Related FMRI: Characterizing Differential Responses," *NeuroImage*, vol. 7, pp. 30-40, 1998.
[38] K. S. Petersen, L. K. Hansen, T. Kolenda, E. Rostrup, and S. C. Strother, "On the Independent Components of Functional Neuroimages," in *Proc. Int. Conf. on ICA and BSS*, Helsinki, Finland, pp. 615-620, 2000.
[39] J. V. Stone, J. Porrill, C. Buchel, and K. Friston, "Spatial, Temporal, and Spatiotemporal Independent Component Analysis of FMRI Data," in *Proc. Leeds Statistical Research Workshop*, Leeds, England, 1999.
[40] V. D. Calhoun, T. Adali, and G. D. Pearlson, "Independent Component Analysis Applied to FMRI Data: A Generative Model for Validating Results," *Journal of VLSI Signal Proc. Systems*, vol. 37, pp. 281-291, 2004.
[41] C. F. Beckmann, J. A. Noble, and S. M. Smith, "Investigating the Intrinsic Dimensionality of FMRI Data for ICA," in *NeuroImage*, vol. 13, p. S76, 2001.
[42] F. Esposito, E. Formisano, E. Seifritz, R. Goebel, R. Morrone, G. Tedeschi, and F. D. Salle, "Spatial Independent Component Analysis of Functional MRI Time-Series: to What Extent Do Results Depend on the Algorithm Used?," *Hum. Brain Map.*, vol. 16, pp. 149-157, 2002.
[43] V. D. Calhoun, T. Adali, J. J. Pekar, and G. D. Pearlson, "Independent Component Analysis Facilitates FMRI of an Naturalistic Behavior: Hypothesized Neural Substrates of Simulated Driving," in *Proc. ISMRM*, Honolulu, HI, 2002.
[44] S. Kullback and R. A. Leibler, "On Information and Sufficiency," *The Annals of Mathematical Statistics*, vol. 22, pp. 79-86, 1951.
[45] N. Correa, T. Adali, Y. Li, and V. D. Calhoun, "Comparison of Blind Source Separation Algorithms for FMRI Using a New Matlab Toolbox: GIFT," in *Proc. IEEE Int. Conf. Acoustics, Speech, Signal Processing (ICASSP)*, Philadelphia, PA, 2005.
[46] S. Cruces, A. Cichocki, and S. Amari, "Criteria for the Simultaneous Blind Extraction of Arbitrary Groups of Sources," in *Proc. Int. Conf. on ICA and BSS*, San Diego, CA, 2001.
[47] L. Tong, V. C. Soon, Y. F. Huang, and R. Liu, "Indeterminacy and Identifiability of Blind Identification," *IEEE Trans. Circuits and Systems*, vol. 38, pp. 499-509, 1991.
[48] V. D. Calhoun, "Group ICA of FMRI Toolbox (GIFT)," http://icatb.sourceforge.net, Released 2004.
[49] A. Cichocki, "ICALAB," http://www.bsp.brain.riken.jp/ICALAB, Released 2002.
[50] V. D. Calhoun, T. Adali, V. McGinty, J. J. Pekar, T. Watson, and G. D. Pearlson, "FMRI Activation In A Visual-Perception Task: Network Of Areas Detected Using The General Linear Model And Independent Components Analysis," *NeuroImage*, vol. 14, pp. 1080-1088, 2001.
[51] M. Svensen, F. Kruggel, and H. Benali, "ICA of FMRI Group Study Data," *NeuroImage*, vol. 16, pp. 551-563, 2002.
[52] D. G. Leibovici and C. F. Beckmann, "An Introduction to Multiway Methods for Multi-Subject FMRI," *FMRIB Technical Report (TR01DL1)*, 2001.
[53] V. J. Schmithorst and S. K. Holland, "Comparison of Three Methods for Generating Group Statistical Inferences From Independent Component Analysis of Functional Magnetic Resonance Imaging Data," *J. Magn Reson. Imaging*, vol. 19, pp. 365-368, 2004.
[54] J. F. Cardoso, "Source Separation Using Higher Order Moments," in *Proc. IEEE Int. Conf. Acoustics, Speech, Signal Processing (ICASSP)*, pp. 2109-2112, 1989.
[55] C. F. Beckmann and S. M. Smith, "Tensorial Extensions of Independent Component Analysis for Multisubject FMRI Analysis," *NeuroImage*, vol. 25, pp. 294-311, 2005.
[56] V. D. Calhoun, T. Adali, G. D. Pearlson, and J. J. Pekar, "A Method for Testing Conjunctive and Subtractive Hypotheses on Group FMRI Data Using Independent Component Analysis," in *Proc. ISMRM*, Toronto, Canada, 2003.
[57] A. S. Lukic, M. N. Wernick, L. K. Hansen, and S. C. Strother, "An ICA Algorithm For Analyzing Multiple Data Sets," in *Int. Conf. on Image Processing (ICIP)*, Rochester, NY, 2002.
[58] V. D. Calhoun, T. Adali, and J. J. Pekar, "A Method for Testing Conjunctive and Subtractive Hypotheses on Group FMRI Data Using Independent Component Analysis," *Mag. Res. Imag.*, vol. 9, pp. 1181-1191, 2004.
[59] V. D. Calhoun, T. Adali, M. Kraut, and G. D. Pearlson, "A Weighted-Least Squares Algorithm for Estimation and Visualization of Relative Latencies in Event-Related Functional MRI," *Magn. Res. Med.*, vol. 44, pp. 947-954, 2000.

[60] M. A. Quigley, V. M. Haughton, J. Carew, D. Cordes, C. H. Moritz, and M. E. Meyerand, "Comparison of Independent Component Analysis and Conventional Hypothesis-Driven Analysis for Clinical Functional MR Image Processing," *AJNR Am. J. Neuroradiol.*, vol. 23, pp. 49-58, 2002.
[61] A. L. Buffington, C. A. Hanlon, and M. J. McKeown, "Acute and Persistent Pain Modulation of Attention-Related Anterior Cingulate FMRI Activations," *Pain*, vol. 113, pp. 172-184, 2005.
[62] C.F.Beckmann, M.De Luca, J.T.Devlin, and S.M.Smith, "Investigations into Resting-State Connectivity Using Independent Component Analysis," to appear *Philos. Trans. R. Soc. Lond B Biol. Sci.*, 2005.
[63] A. Bartels and S. Zeki, "Brain Dynamics During Natural Viewing Conditions-A New Guide for Mapping Connectivity in Vivo," *Neuroimage.*, vol. 24, pp. 339-349, 2005.
[64] V. D. Calhoun, J. J. Pekar, and G. D. Pearlson, "Alcohol Intoxication Effects on Simulated Driving: Exploring Alcohol-Dose Effects on Brain Activation Using Functional MRI," *Neuropsychopharmacology*, vol. 29, pp. 2097-2107, 2004.
[65] W. Lu and J. C. Rajapakse, "ICA With Reference," in *Proc. Int. Conf. on ICA and BSS*, San Diego, CA, pp. 120-125, 2001.
[66] W. Lu and J. C. Rajapakse, "Eliminating Indeterminacy in ICA," *Neurocomputing*, vol. 50, pp. 271-290, 2003.
[67] J. V. Stone, J. Porrill, N. R. Porter, and I. D. Wilkinson, "Spatiotemporal Independent Component Analysis of Event-Related FMRI Data Using Skewed Probability Density Functions," *Neuroimage.*, vol. 15, pp. 407-421, 2002.
[68] J. R. Duann, T. P. Jung, W. J. Kuo, T. C. Yeh, S. Makeig, J. C. Hsieh, and T. J. Sejnowski, "Single-Trial Variability in Event-Related BOLD Signals," *Neuroimage.*, vol. 15, pp. 823-835, 2002.
[69] P. Hojen-Sorensen, O. Winther, and L. K. Hansen, "Analysis of Functional Neuroimages Using ICA Adaptive Binary Sources," *Neurocomputing*, vol. 49, pp. 213-224, 2002.
[70] R. A. Choudrey and S. J. Roberts, "Flexible Bayesian Independent Component Analysis for Blind Source Separation," in *Proc. Int. Conf. on ICA and BSS*, San Diego, CA, 2001.
[71] B. Hong and V. D. Calhoun, "Source Density Driven Adaptive Independent Component Analysis Approach for FMRI Signal Analysis," in *Proc. MLSP*, 2004.
[72] M. Welling and M. Weber, "A Constrained EM Algorithm for Independent Component Analysis," *Neural Comput.*, vol. 13, pp. 677-689, 2001.
[73] V. D. Calhoun, T. Adali, G. D. Pearlson, P. C. van Zijl, and J. J. Pekar, "Independent Component Analysis of FMRI Data in the Complex Domain," *Magn Reson. Med.*, vol. 48, pp. 180-192, 2002.
[74] V. D. Calhoun and T. Adali, "Complex ICA for FMRI Analysis: Performance of Several Approaches," in *Proc. ICASSP*, Hong Kong, China, 2003.
[75] V. D. Calhoun, T. Adali, G. D. Pearlson, and J. J. Pekar, "On Complex Infomax Applied to Complex FMRI Data," in *Proc. ICASSP*, Orlando, FL, 2002.

LEGENDS

Figure 1.1: (a) The joint density of two independent signals, (b) PCA projection (u_1, u_2), (c) ICA projection (a_1, a_2) (adopted from [1])

Figure 1.2: Basic ICA model for blind source separation

Figure 2.1: Motion-related signal due to mouth movement from inferior temporal and orbitofrontal regions

Figure 3.1: Comparison of GLM and ICA (left) and ICA illustration (right). The GLM (top left) is by far the most common approach to analyzing fMRI data, and to use this approach, one needs a model for the fMRI time course whereas in spatial ICA (bottom left), there is no explicit temporal model for the fMRI time course, this is estimated along with the hemodynamic source locations. (right) The ICA model assumes the fMRI data, x, is a linear mixture of statistically independent sources, s and the goal of ICA is to separate the sources given the mixed data and thus determine the s and A matrices

Figure 3.2: Model for applying ICA to fMRI data

Figure 3.3: (a,b,c) Hybrid-fMRI experiment in which a known source is added to a real fMRI experiment (from [29]). (d) Comparison of algorithms and preprocessing using hybrid data.

Figure 3.4: FMRI single slice results (left visual cortex)

Figure 3.5: fMRI Group ICA results (from [19])

Figure 3.6: Visual, motor, and visuomotor data comparisons (from [58])

Figure 3.7: (left) Mean activation maps from patients with schizophrenia and healthy controls. Right auditory cortex demonstrated the greatest difference (white box); (middle) Right auditory cortex difference maps with optimized boundaries; (right) Individual classification results for cohort 1, and replication in cohort 2. Schizophrenia classification is indicated with the color red.

Figure 3.8: Driving-related networks and their associated time courses compared while sober and at two doses of alcohol.

Figure 3.9: Comparison between Source Density-Driven ICA and Infomax ICA

Figure 3.10: Comparison of ICA and sbICA in one participant

Figure 3.11: Results from magnitude-only analysis (a) and complex-valued analysis (b,c,d).

Figure 1.1

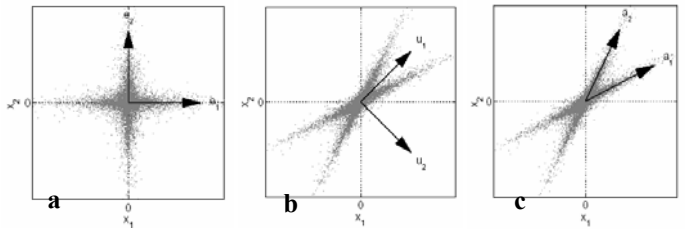

Figure 1.2

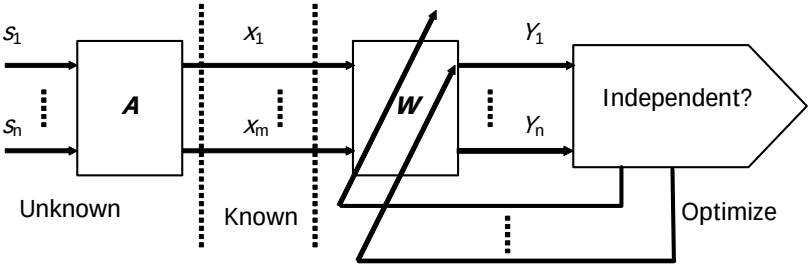

Figure 2.1

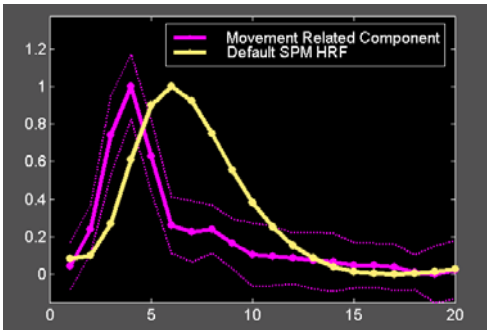
Movement Related Component
Default SPM HRF
1.2
1
0.8
0.6
0.4
0.2
0
0
5
10
15
20

Figure 3.1

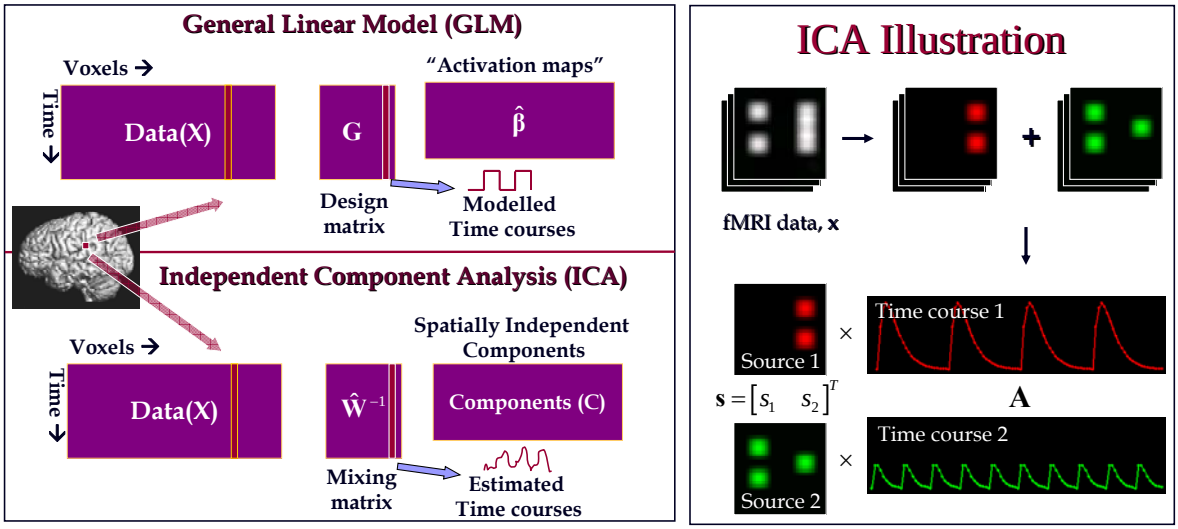
General Linear Model (GLM)
Voxels
Time
Data(X)
G
"Activation maps"
β̂
Design matrix
Modelled Time courses
Independent Component Analysis (ICA)
Voxels
Time
Data(X)
Ŵ⁻¹
Spatially Independent Components
Components (C)
Mixing matrix
Estimated Time courses
ICA Illustration
fMRI data, x
Source 1
Time course 1
s = [s1 s2]T
A
Source 2
Time course 2

Figure 3.2

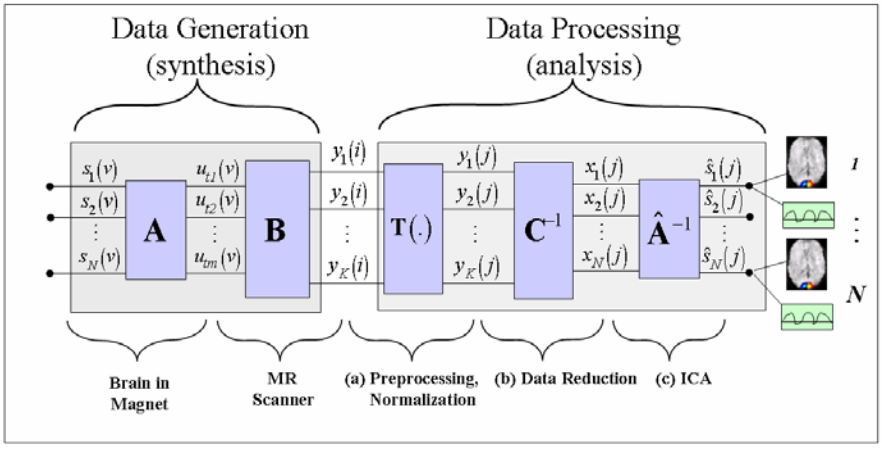
Data Generation
(synthesis)
Data Processing
(analysis)
A
B
T(.)
C^-1
Â^-1
1
N
Brain in
Magnet
MR
Scanner
(a) Preprocessing,
Normalization
(b) Data Reduction
(c) ICA

Figure 3.3

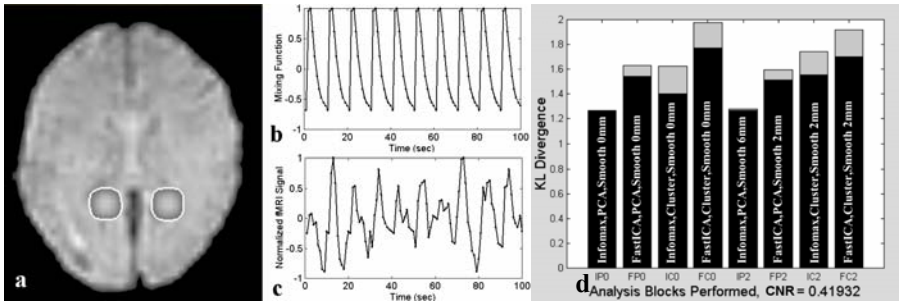
a
b
Mixing Function
Time (sec)
c
Normalized fMRI Signal
Time (sec)
d
KL Divergence
Infomax,PCA,Smooth 0mm
FastICA,PCA,Smooth 0mm
Infomax,Cluster,Smooth 0mm
FastICA,Cluster,Smooth 0mm
Infomax,PCA,Smooth 6mm
FastICA,PCA,Smooth 2mm
Infomax,Cluster,Smooth 2mm
FastICA,Cluster,Smooth 2mm
IP0
FP0
IC0
FC0
IP2
FP2
IC2
FC2
Analysis Blocks Performed, CNR = 0.41932

Figure 3.4

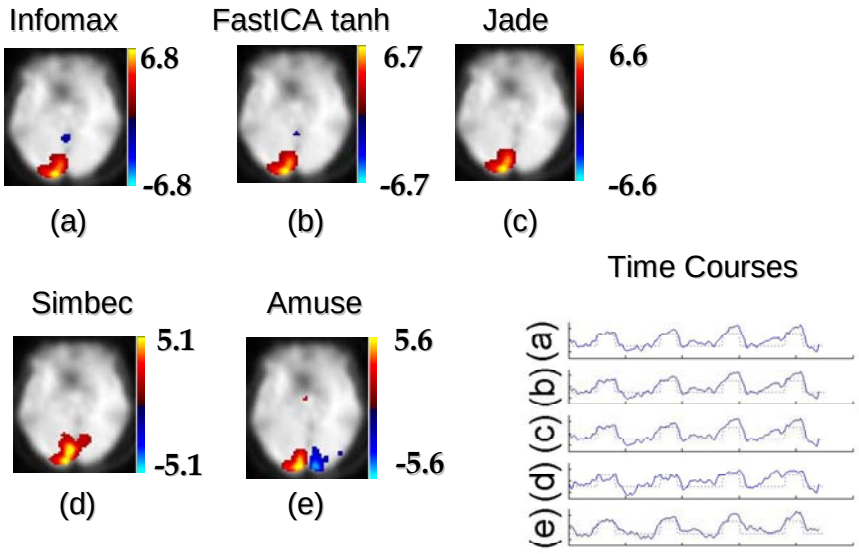
Infomax
6.8
-6.8
(a)
FastICA tanh
6.7
-6.7
(b)
Jade
6.6
-6.6
(c)
Simbec
5.1
-5.1
(d)
Amuse
5.6
-5.6
(e)
Time Courses
(a)
(b)
(c)
(d)
(e)

Figure 3.5

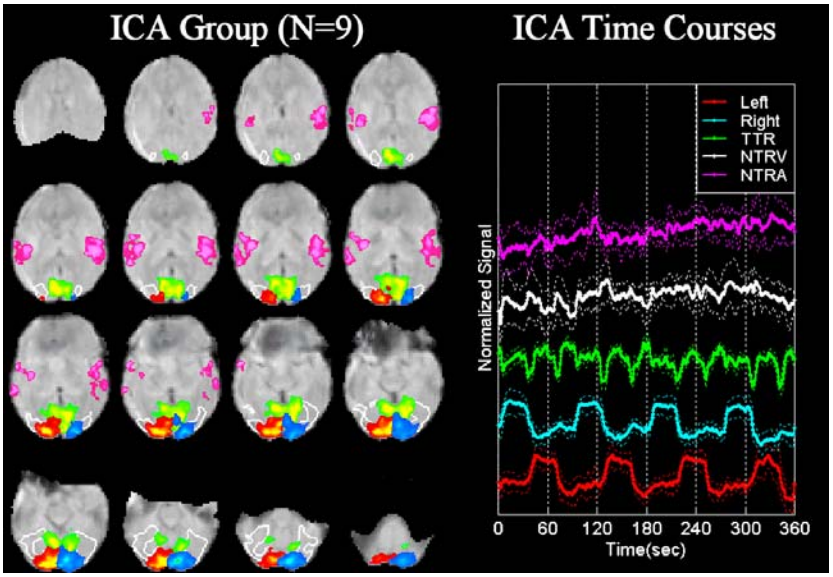
ICA Group (N=9)
ICA Time Courses
Left
Right
TTR
NTRV
NTRA
Normalized Signal
0
60
120
180
240
300
360
Time(sec)

Figure 3.6

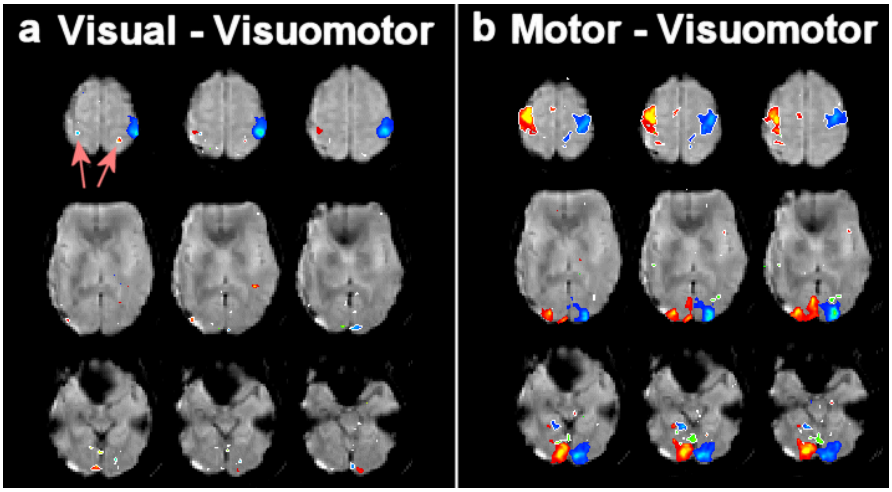

Figure 3.7

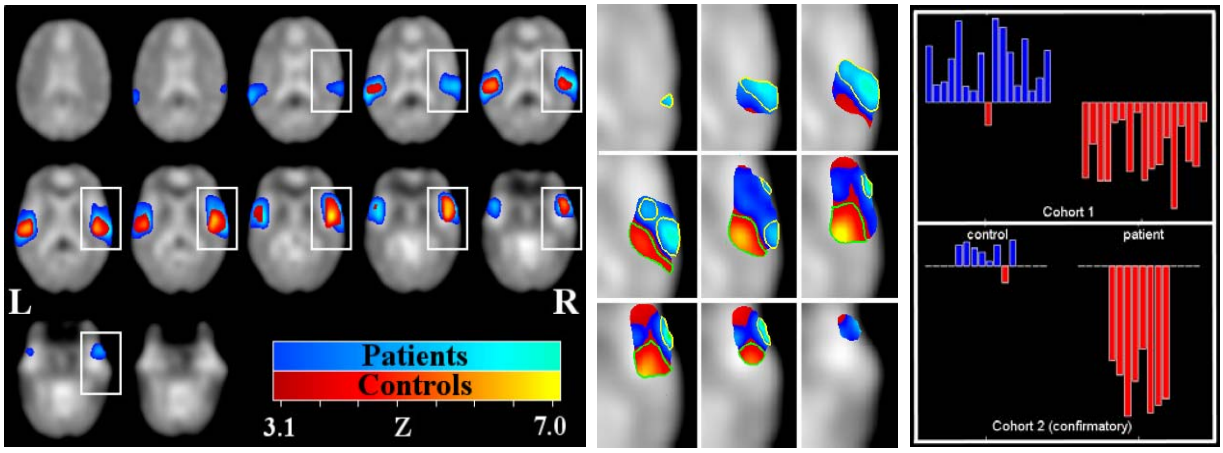
L
R
Patients
Controls
3.1
Z
7.0
Cohort 1
control
patient
Cohort 2 (confirmatory)

Figure 3.8

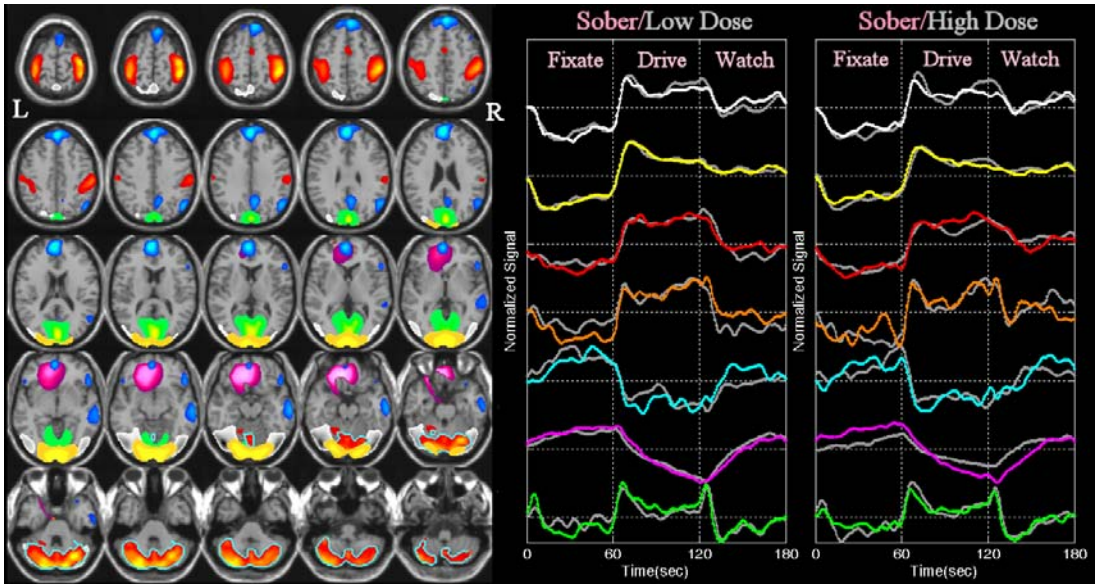
L
R
Sober/Low Dose
Fixate
Drive
Watch
Normalized Signal
0
60
120
180
Time(sec)
Sober/High Dose
Fixate
Drive
Watch
Normalized Signal
0
60
120
180
Time(sec)

Figure 3.9

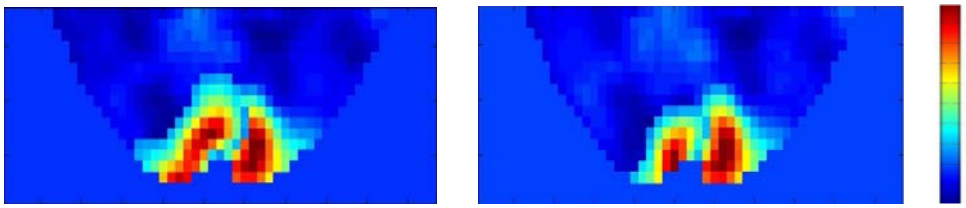

(a) Source Density-Driven ICA (b) Infomax ICA

Figure 3.10

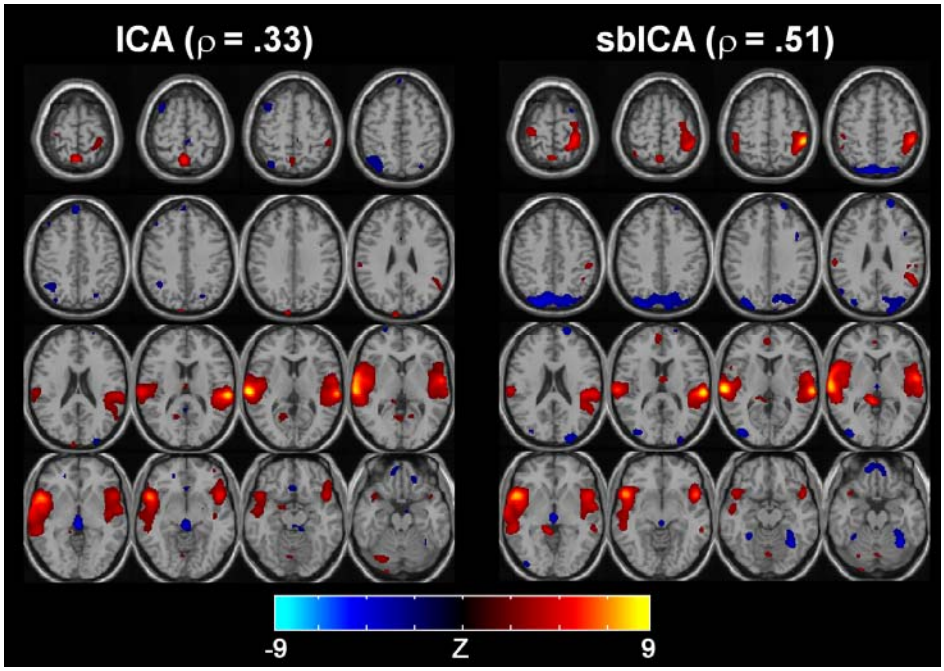

Figure 3.11

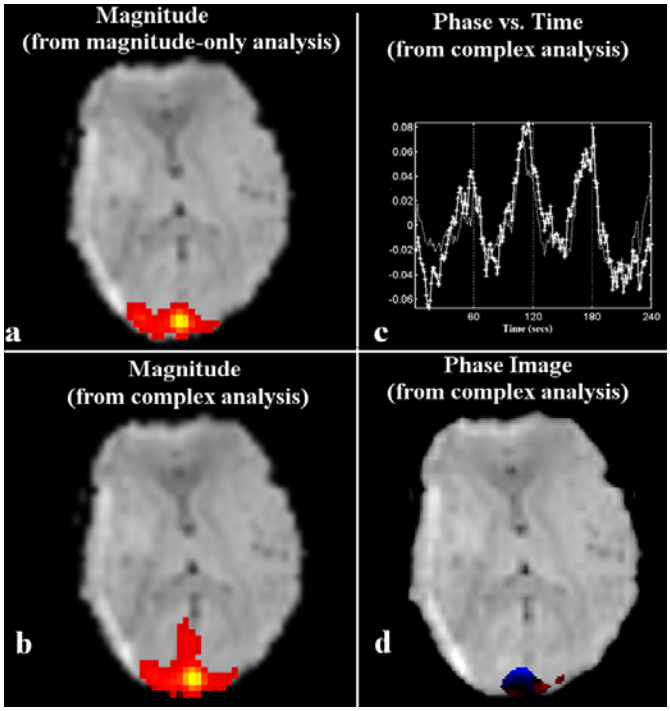
Magnitude
(from magnitude-only analysis)
a
Phase vs. Time
(from complex analysis)
0.08
0.06
0.04
0.02
0
-0.02
-0.04
-0.06
60
120
180
240
Time (secs)
c
Magnitude
(from complex analysis)
b
Phase Image
(from complex analysis)
d